

# Helheim velocity controlled both by terminus effects and subglacial hydrology with distinct realms of influence

A.N. Sommers<sup>1</sup>, C.R. Meyer<sup>1</sup>, K. Poinar<sup>2</sup>, J. Mejia<sup>2</sup>, M. Morlighem<sup>1</sup>, H.  
Rajaram<sup>3</sup>, K.L.P. Warburton<sup>1</sup>, W. Chu<sup>4</sup>

<sup>1</sup>Dartmouth College, Hanover, NH, USA

<sup>2</sup>University at Buffalo, Buffalo, NY, USA

<sup>3</sup>Johns Hopkins University, Baltimore, MD, USA

<sup>4</sup>Georgia Institute of Technology, GA, USA

## Key Points:

- We couple a subglacial hydrology model with an ice flow model to simulate the relationship between sliding velocity and effective pressure.
- Terminus effects at Helheim Glacier drive velocity up to 15 km upstream, but seasonal hydrology controls velocity patterns further inland.
- Increased melt accelerates ice inland of the main trunk, implying importance of hydrology in tidewater glacier future mass balance.

---

Corresponding author: Aleah Sommers, [Aleah.N.Sommers@dartmouth.edu](mailto:Aleah.N.Sommers@dartmouth.edu)

## Abstract

Two outstanding questions for future Greenland predictions are (1) how enhanced meltwater draining beneath the ice sheet will impact the behavior of large tidewater glaciers, and (2) to what extent tidewater glacier velocity is driven by changes at the terminus versus changes in sliding velocity due to meltwater input. We present a two-way coupled framework to simulate the nonlinear feedbacks of evolving subglacial hydrology and ice dynamics using the Subglacial Hydrology And Kinetic, Transient Interactions (SHAKTI) model within the Ice-sheet and Sea-level System Model (ISSM). Through coupled simulations of Helheim Glacier, we find that terminus effects dominate the seasonal velocity pattern up to 15 km from the terminus, while hydrology primarily drives the velocity response upstream. With increased melt, the hydrology influence yields seasonal acceleration of several hundred meters per year in the interior, suggesting that hydrologic forcing will play an important role in future mass balance of tidewater glaciers.

## Plain Language Summary

Water draining under glaciers and ice sheets affects the friction between the ice and the bed, and controls how fast the ice can slide into the ocean, contributing to sea-level rise. We present a framework for simulating the feedbacks between hydrology and ice flow. We investigate the relative influence of changes at the terminus of the glacier where it meets the ocean, versus changes in meltwater drainage, in determining how fast the glacier moves. Our modeling of Helheim Glacier in southeast Greenland highlights the importance of terminus effects up to 15 km from the terminus, and hydrology farther upstream, with increased melt yielding higher inland acceleration. These results suggest that meltwater will play an increasingly important role in the future behavior of glaciers.

## 1 Introduction

The Greenland Ice Sheet is losing mass at an accelerating rate (Mouginot et al., 2019; Mankoff et al., 2020), with the majority of ice lost via large tidewater glaciers. A persistent unknown in the evolution of the ice sheet is the relative influence on tidewater glacier behavior by near-terminus effects at the ice–ocean interface versus effects of seasonal meltwater draining to the bed (Cheng et al., 2022; Cook et al., 2020, 2022; Stevens et al., 2018, 2022a, 2022b; Ultee et al., 2022). The spatial regions influenced by these competing effects, and their balance or imbalance, remain uncertain in both the current and future states of the ice sheet, as glaciers retreat and melt increases.

The subglacial environment is difficult to access; few boreholes have been drilled to the bed of tidewater glaciers. Ice flow and hydrology models can provide estimates of basal stresses and water pressure under a range of conditions, rendering a process for calculating sliding velocities. Two-way coupling between hydrology and ice dynamics models is necessary because the subglacial drainage geometry and water pressure are influenced by ice sliding velocity as frictional heat causes melt, and the sliding velocity is in turn modulated by basal stresses and water pressure. Several approaches exist for simulating different aspects of the subglacial drainage system (Flowers, 2015; de Fleurian et al., 2018). Previous efforts have developed coupled models with varying complexity, and this remains an active area of research (Arnold & Sharp, 2002; Pimentel & Flowers, 2011; Hewitt, 2013; Kingslake & Ng, 2013; Hoffman & Price, 2014; Gagliardini & Werder, 2018; Drew & Tarasov, 2023; Ehrenfeucht et al., 2023; Lu & Kingslake, 2023).

In this paper, we implement an innovative two-way coupled modeling framework to simulate subglacial hydrology and ice dynamics using the Subglacial Hydrology And Kinetic, Transient Interactions model (SHAKTI; Sommers et al., 2018, 2023) in the Ice-sheet and Sea-level System Model (ISSM; Larour et al., 2012). We investigate the relative influence of hydrology and terminus effects in driving the seasonal velocity cycle

along the length of Helheim Glacier in southeast Greenland. In what follows, we describe the modeling methods and experimental setup, interpret results, and discuss implications of our findings.

## 2 Methods

### 2.1 Model description

We simulate the subglacial hydrological system with the SHAKTI model as described by Sommers et al. (2018), specifically using the reduced SHAKTI model presented by Sommers et al. (2023), involving a minimal number of unknown parameters. SHAKTI solves a set of nonlinear equations based on mass, momentum, and energy balances, along with opening due to melt and closing of the subglacial system due to ice creep. These equations calculate hydraulic head (from which water pressure and effective pressure are readily obtained), basal water flux, and geometry of the drainage system. Hydraulic transmissivity varies temporally and spatially and is calculated as a function of the local Reynolds number. Basal water flux accommodates both laminar and turbulent flow, along with smooth transitions between these regimes, a feature that has been shown to more accurately represent observed pressures than the common assumption of fully laminar or fully turbulent flow (Hill et al., 2023).

ISSM is a state-of-the-art ice sheet model that simulates ice flow over a wide range of scales and applications (Larour et al., 2012). In the simulations presented in this study, ice thickness and terminus position are unchanging. We use the Shallow-Shelf Approximation (SSA) to calculate ice velocity. The assumption of negligible vertical shear invoked in SSA is a valid approach for fast-moving outlet glaciers where velocity can be assumed to be primarily due to basal sliding. While SSA may not be as justifiably valid in the slower-moving inland portions of Helheim, coupled model tests using the depth-integrated higher order stress balance module (MOLHO, Dias dos Santos et al. (2022)) instead of SSA produce only minor differences in results (Figs. S1 and S2). SSA involves a depth-integrated value for the flow law parameter (related to ice viscosity). We use a value corresponding to ice at  $-10^{\circ}\text{C}$ ; sensitivity tests using  $-15^{\circ}\text{C}$  instead yield small differences in modeled winter velocity and effective pressure (Figs. S3 and S4).

SHAKTI is built as a hydrology module into ISSM. Simulations presented in this paper couple SHAKTI with the stress balance solver for the first time. SHAKTI and the stress balance solver are coupled in an alternating manner through effective pressure at the bed (the difference between ice overburden pressure and water pressure, calculated by SHAKTI) and ice sliding velocity (calculated by the stress balance solver). Several different methods of representing basal friction and sliding are available as model options within ISSM; simulations presented in this paper use a Budd-type sliding law (Budd et al., 1979), with basal shear stress  $\tau_b$  calculated as

$$\tau_b = C^2 N^{q/p} |\mathbf{u}_b|^{1/p}, \quad (1)$$

which involves a spatially variable drag coefficient  $C$ , along with spatially and temporally variable effective pressure  $N$  and sliding velocity  $\mathbf{u}_b$ . The friction exponents used in this study are  $p = 1$  and  $q = 1$ . SHAKTI uses the sliding velocity from the stress balance to calculate the basal melt rate due to frictional heat from sliding, and the stress balance solver uses the effective pressure calculated by SHAKTI in the viscous friction basal boundary condition to compute the ice velocity. As the basal stress  $\tau_b$  depends on both effective pressure and sliding velocity, Eqn. 1 essentially becomes a nonlinear equation for calculating  $u_b$ . In the stress balance solver, a limit is imposed in the calculation of  $\tau_b$  such that  $N = \max(N, 0)$  and no negative basal stress is possible.

## 2.2 Study site

Helheim Glacier is a fast-moving tidewater glacier in southeast Greenland (Fig. 1b). Our model domain covers  $5.6 \times 10^3$  km<sup>2</sup> of the Helheim glaciologic and hydrologic catchment, extending up to over 2000 m surface elevation and capturing the two main ice flow branches as well as smaller tributaries (Figure S5). We discretize the model domain using an unstructured triangular mesh consisting of 27,913 elements, refined according to observed ice velocity (Joughin et al., 2018) (Figure S6). Element edge lengths range from 70 m near the terminus to 2500 m in the slower-moving interior. Ice geometry (bed topography and surface elevation) is drawn from the BedMachine v4 dataset (Morlighem et al., 2021).

We subdivide Helheim Glacier into three regions as defined by their surface elevation (Figure 1b). Region 1, extending from the terminus up to surface elevation 900 m above sea level, is the most heavily crevassed and fastest moving portion of the glacier where the northern and southern branches meet. Region 2 is the intermediate zone extending from 900 to 1500 m elevation, characterized by shallower surface slopes and moderate crevassing. Region 3 extends from 1500 m elevation to the upper edge of our domain and encompasses the firn aquifer area (Miège et al., 2016), with the downstream boundary containing the crevasse fields that drain the firn aquifer.

## 2.3 Boundary conditions

In SHAKTI, we set a Dirichlet boundary condition along the glacier terminus to prescribe hydraulic head so that the water pressure of subglacial discharge is equal to the overlying hydrostatic pressure of the water in the fjord. At all other boundaries, we employ a Neumann boundary condition to prescribe zero water flux. Additionally, we set the water pressure under any areas with ice thickness of 10 m or less to be equal to atmospheric pressure.

For the ice dynamics in ISSM, a stress-free boundary condition is assumed at the ice surface, with a viscous friction law applied at the bed. Observed ice velocity is prescribed as a Dirichlet boundary condition at the model domain edges. We deliberately define a large domain with low velocities at all boundaries. At the terminus, water pressure is applied for a force balance at the ice–ocean interface. Velocity everywhere within the model domain evolves freely – with the exception of some simulations described below that involve terminus forcing, in which a time-varying velocity is prescribed as a transient Dirichlet boundary condition at the ice–ocean interface.

## 2.4 Coupled winter simulation

To generate an initial state of the subglacial hydrological system, we perform a coupled SHAKTI-ISSM spin-up simulation to steady state under “winter” conditions, with no meltwater input to the bed from the surface or englacial system, i.e. assuming all water is generated through basal melt, as in the stand-alone SHAKTI simulations by Sommers et al. (2023).

A typical approach in ISSM simulations without an evolving hydrology model is to use inverse methods to match observed velocity by optimizing the basal drag coefficient  $C$  involved in the basal stress calculation (Eqn. 1). This requires some assumption of effective pressure at the bed, which is commonly assumed in such inversions to be represented with total connectivity to the ocean. This may be a reasonable approximation close to the ice–ocean boundary, but is incorrect further upstream under thick ice at great distances from the ocean (Minchew et al., 2019). Using a drag coefficient distribution obtained through inversion assuming this static effective pressure yields velocities in coupled SHAKTI-ISSM that diverge significantly from observations in portions of the model domain. In many uncoupled ice-sheet model simulations, the drag coefficient typically

serves as a catch-all tuning factor intended to represent several basal conditions, including corrections to the simplified effective pressure assumption. Since SHAKTI explicitly calculates effective pressure, however, this must be separated from the drag coefficient.

We produce a drag coefficient distribution (Fig. S7) via an iterative inversion and spin-up method (Fig. S8). We first invert for basal drag with assumed effective pressure, then use the resulting drag field in a coupled SHAKTI-ISSM winter simulation for 30 days with a time step of one hour, yielding a new effective pressure field, which then goes into a subsequent ISSM inversion for drag. This drag field seeds a final SHAKTI-ISSM spin-up simulation for 30 days plus one year to adequately reach steady state, creating the initial winter conditions to serve as the background “base state” for the seasonal simulations described below (Figure S9). Parameter and constant values used in the simulations are given in Table S1.

## 2.5 Coupled seasonal experiments

To examine the relative influence of seasonal hydrology and terminus effects in controlling the seasonal velocity behavior of Helheim Glacier, we conduct several SHAKTI-ISSM simulations with transient forcing. Table S2 presents a summary of the simulations. Each simulation is forced by different meltwater inputs to the bed, terminus velocity changes, or both.

### 2.5.1 Seasonal hydrology forcing

Beginning from the winter base state obtained through the coupled model spin-up described above, we apply seasonal hydrology forcing as transient meltwater inputs to the bed. In the spirit of Poinar et al. (2019), we specify meltwater inputs according to three distinct regions based on surface elevation as described above (Figure 1b). In Region 1, we supply water to the bed in a distributed manner, with magnitude and timing prescribed by 2018 reanalysis data (GMAO, 2015) smoothed with a 14-day running average, at the  $56 \text{ km} \times 27 \text{ km}$  grid cell centered at  $66.50^\circ\text{N}$ ,  $38.15^\circ\text{W}$ , which overlaps the Helheim terminus (Poinar, 2023). Given that this lower region of Helheim is heavily crevassed, surface meltwater does not necessarily reach the bed through isolated point inputs such as moulins, as in western Greenland. Accordingly, we approximate low-elevation meltwater inputs as distributed evenly over the bed to represent widespread crevassing. The meltwater input rate over Region 1 in our *seasonal* simulation varies from  $0\text{--}6.7 \text{ m yr}^{-1}$  (Fig. 1a), with a total annual volume of  $3.5 \times 10^{20} \text{ m}^3$  distributed input to the bed. In Region 2, we follow Poinar et al. (2019) and assume that local meltwater percolates into the firn and refreezes without reaching the bed. In our *enhanced melt* simulations, however, we consider meltwater inputs to the bed in Region 2, with meltwater input rate varying from  $0\text{--}13.4 \text{ m yr}^{-1}$  over both Regions 1 and 2 (Fig. 1a), yielding an annual distributed meltwater input volume of  $2.4 \times 10^{21} \text{ m}^3$ . For Region 3, we assume that surface meltwater is retained as englacial liquid water in the firn aquifer, which then drains through crevasses at the downstream edge of the firn aquifer at approximately the 1500 m elevation line. We apply steady drainage from this inland firn aquifer into point inputs to represent disparate crevasses. A total of  $50 \times 10^6 \text{ m}^3 \text{ yr}^{-1}$  is divided evenly among 64 “firn aquifer crevasse drainage” points at those finite element vertices located between 1500–1515 m above sea level (Figs. 1b and S6), at a steady rate of  $0.0248 \text{ m}^3 \text{ s}^{-1}$  reaching the bed at each point. In our *enhanced melt* simulations, this firn aquifer input rate is doubled to  $0.0495 \text{ m}^3 \text{ s}^{-1}$  for an annual volume of  $100 \times 10^6 \text{ m}^3$ .

### 2.5.2 Terminus forcing

To represent the influence of effects at the ice terminus, we apply a transient Dirichlet velocity boundary condition to the terminus with a shape inspired by 2018 observa-

tions near the terminus of Helheim Glacier (ITS-LIVE, Fig. S10a), which we approximate as a sinusoidal curve in time, with a period of one year, that varies  $\pm 1000 \text{ m yr}^{-1}$  around the simulated winter base velocity of each element edge along the terminus, peaking on Day 92 (April 2) with minimum on Day 275 (October 2). This method of prescribing velocity at the terminus aims to capture the lumped impact of such factors as buttressing from ice mélange in the fjord, calving, changes in terminus position, tidal movement, and other ocean-ice interactions. This forcing allows us to determine the relative influence of terminus effects on catchment-scale velocity as compared to hydrology, without specific attribution between individual processes playing out at the terminus.

### 3 Results

Below are results of coupled SHAKTI-ISSM simulations forced by seasonal hydrology, terminus effects, and both. We focus our attention on model output of velocity and effective pressure fields through time and space in the various simulations.

#### 3.1 Hydrology-forced results

Figure 1 presents results of effective pressure and ice velocity in the SHAKTI-ISSM simulations forced by seasonal meltwater inputs with freely evolving terminus velocity (*seasonal*, *seasonal+firn aquifer*, *enhanced melt*). The temporal sequencing of seasonal peak in meltwater input, minimum effective pressure, and maximum velocity varies by location, indicative of the nonlinear and nonlocal coupling effects.

Near the terminus (point A in Figure 1b), peak velocity occurs on day 156, before minimum effective pressure (i.e. peak basal water pressure) on day 163, and the velocity-effective pressure relationship exhibits a marked hysteresis loop (Figure 1c-e). The *enhanced melt* simulation displays a double peak in velocity (Fig. 1d).

At the confluence of the two main ice flow branches of Helheim (point B; Figure 1f-g), minimum effective pressure occurs first (day 151), followed by peak velocity six days later, both occurring before peak meltwater input on day 163 (Figure 1a). The period just before peak velocity corresponds to negative effective pressure at this location. This sequence may be understood through the traditional concept of channelization or development of more efficient drainage during a melt season: as the melt season initiates, the system becomes pressurized, leading to ice acceleration, but continued meltwater inputs trigger a shift to localized higher-capacity flow paths with higher gap height (Fig. S11a,b), by which water is efficiently drained from the surrounding bed, lowering water pressure and sliding velocity by increasing friction. Velocity and effective pressure at the confluence display an unusual figure-eight shaped hysteresis relationship (Figure 1h). In the *enhanced melt* simulation, peak velocity precedes minimum effective pressure, and both occur even earlier (days 144 and 148, respectively; Figure 1f-g), with a double peak in velocity and heavy channelization by peak meltwater input (Fig. S11c,d).

Upstream along the northern branch (point C), minimum effective pressure and peak velocity occur on days 154 and 156, respectively (Figure 1i-j). Further upstream on the southern branch (point D), low-elevation seasonal meltwater input leads to only minor changes in effective pressure and velocity (Figure 1l-n). With *enhanced melt* (higher magnitude and at higher elevation), the response is greater in both effective pressure and velocity, with lower effective pressure corresponding to higher velocity (yellow line in Figure 1l-m). Interestingly, the hysteresis loop for point D (Fig. 1n) has a positive slope whereas the loops for other downstream points have negative slopes (Figs. 1e, h, k). At this upstream point on the southern branch, higher velocity corresponds to higher effective pressure in the *seasonal* and *seasonal+firn aquifer* simulations, reflecting nonlocal behavior, i.e. influence from changes in the surrounding area as a result of the sliding law. These variations in velocity and effective pressure are very small, however. In the *enhanced melt*



simulation, the increased presence of meltwater at the bed renders a hysteresis loop at point D with a negative slope like the other points (Fig. S12), in which higher velocity corresponds to lower effective pressure, showing that more melt corresponds to more locally-driven behavior.

Steady year-round inputs of meltwater to the bed from the firn aquifer draining through crevasses as simulated here (*seasonal+firn aquifer*) have a minor influence on downstream velocity compared to low-elevation seasonal meltwater only (*seasonal*). This small effect is visible as the difference between the blue and red-dashed lines in Fig. 1. The most notable impact of including firn aquifer inputs is the consistently higher ice velocities, particularly outside of the melt season.

The late-season event centered around day 250 in the meltwater input (Fig. 1a) affects pressure and velocity at all our points of interest in Fig. 1, with an outsized effect in the *enhanced melt* simulation. As a result of the drainage system shutting down at the end of the primary melt season, the additional spike of late-season meltwater delivered to the bed causes a heightened pressurization and acceleration.

When forced by seasonal meltwater inputs, an annual minimum velocity occurs at points A (terminus) and B (confluence) in the late melt season (Figure 1d,g), a pattern typically associated with hydrology-driven velocity behavior (Moon et al., 2014), when meltwater inputs into an efficient drainage network decrease. Velocity observations, however, do not show such a minimum at Helheim (Fig. S10a,b), reaffirming that the system is not purely controlled by hydrology, especially near the terminus, in agreement with conclusions of other studies (Moon et al., 2014; Cheng et al., 2022; Ultee et al., 2022; Poinar, 2023).

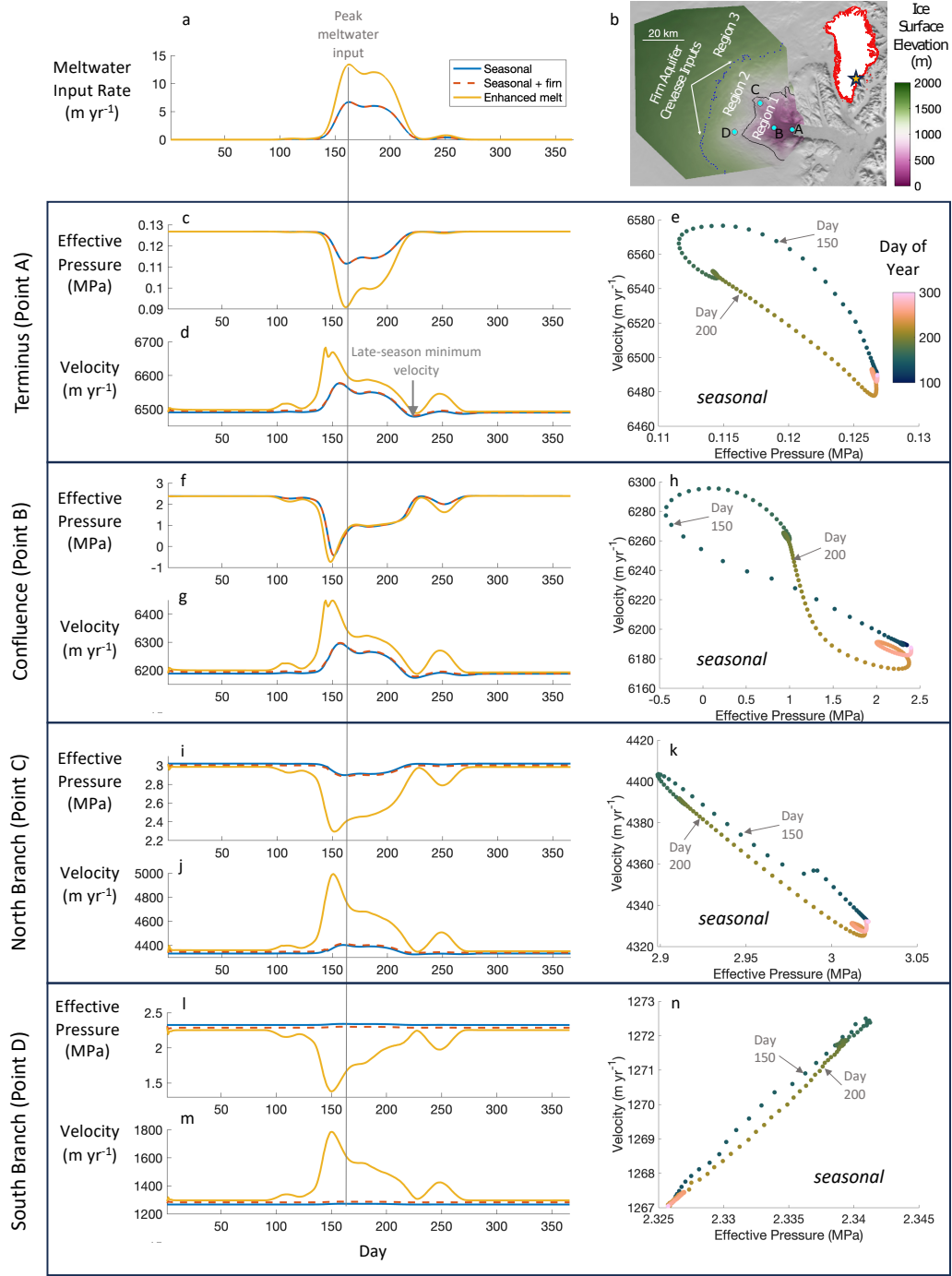
### 3.2 Terminus-forced results

Results of our SHAKTI-ISSM simulation forced by an applied transient velocity at the terminus (*termforce*) suggest that terminus effects carry a strong influence on velocity in the main trunk of the glacier up to approximately 15 km inland from the terminus (Figures 2 and S13). The impact of terminus forcing on ice velocity further inland is weak.

### 3.3 Hydrology- and terminus-forced results

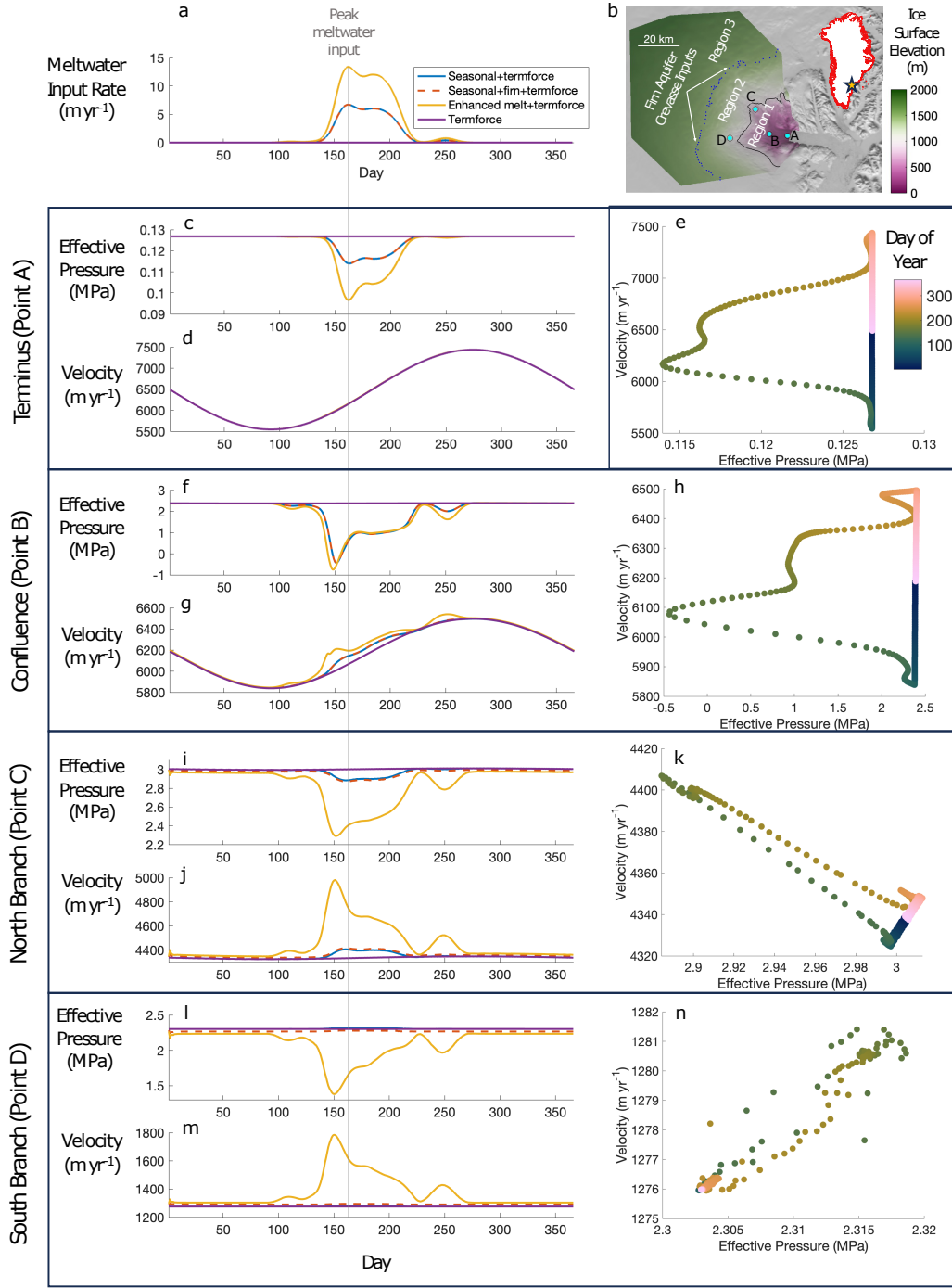
We combine seasonal meltwater inputs and terminus forcing to examine the influence of each at different locations in the glacier (Figure 2). In general, terminus effects largely control the velocity pattern in the main trunk, from the terminus to about 15 km upstream (Figure 2d,g). The seasonality of melt inputs controls variations in effective pressure (Figure 2c,f,i,l) and is the dominant control on velocity further inland (Figure 2j,m). In the *enhanced melt+termforce* simulation, the influence of seasonal meltwater on velocity becomes stronger at the confluence (Figure 2g) along with greater seasonal acceleration in the interior (Figure 2j,m).

Figure 3 presents the change in sliding velocity and effective pressure with respect to the winter base state on the day of minimum terminus velocity (April 2 / day 92), maximum meltwater input to the bed (June 12 / day 163), and maximum terminus velocity (October 2 / day 275), for our *seasonal+firn aquifer+termforce* and *enhanced melt+termforce* simulations. The 15-km inland extent of strong terminus forcing is displayed through the change in velocity on days 92 and 275, outside of the melt season (Figure 3a,c,g,i), and in the presence of melt (Fig. 3b,h), with a coupling length that emerges from ice physics and local geometry (Enderlin et al., 2016). Although the main trunk has a lower velocity compared to winter due to the terminus forcing on the day of peak meltwater input (June 12 / day 163), the tributary branches of the glacier show a marked increase in velocity at peak melt as a result of seasonal meltwater reaching the bed (Figure 3b). This



**Figure 1.** Results of coupled simulations forced by seasonal meltwater: a) Seasonal meltwater input rate. b) Mapped location of points of interest overlaid on ice surface elevation and meltwater input regions. Inset: location of Helheim Glacier in southeast Greenland shown by star. c-n) Effective pressure and ice velocity time series results for all three meltwater-forced SHAKTI-ISSM simulations (*seasonal*, *seasonal+firn aquifer*, *enhanced melt*). Sub-plots e, h, k, and n show velocity versus effective pressure in the *seasonal* simulation with colors corresponding to the colorbar in e. Note that the axis ranges differ across panels.





**Figure 2.** Results of simulations forced by both seasonal meltwater and terminus velocity: a) Seasonal meltwater input rate. b) Mapped location of points of interest overlaid on ice surface elevation and meltwater input regions. Inset: location of Helheim Glacier in southeast Greenland shown by star. c-n) Effective pressure and ice velocity time series results for all three meltwater-and-terminus-forced SHAKTI-ISSM simulations (*seasonal+termforce*, *seasonal+firn aquifer+termforce*, *enhanced melt+termforce*), Sub-plots e, h, k, and n show velocity versus effective pressure in the *seasonal+termforce* simulation. Note that the axis ranges are different.

effect is amplified in the *enhanced melt+termforce* simulation (Figure 3h), which shows a greater acceleration further upstream and reduced influence from terminus forcing at the confluence of the two main ice flow branches. Effective pressure is lower (i.e. water pressure is higher) than the winter base state in the region of meltwater inputs during the peak melt season, producing a distinct band of increased effective pressure (i.e. lower water pressure) located just upstream of the meltwater input extent, i.e. the inland boundary of Region 1 (Figure 3e). The width of this band and its magnitude of change relative to winter are greater in the *enhanced melt+termforce* simulation, upstream of the meltwater input extent in this case, i.e. the inland boundary of Region 2 (Figure 3k).

One may wonder whether the effects on velocity due to terminus forcing and hydrology forcing are simply additive. Velocity results from the simulation with combined forcing are weakly nonlinear as compared to the simulations with only either hydrology or terminus forcing, especially during peak melt season, yielding slightly lower velocity (<0.4%) than the sum of the terminus-only and melt-only simulations (Fig. S14).

## 4 Discussion

### 4.1 Velocity patterns at Helheim driven by both terminus effects and runoff

Motivated to understand glacier velocity patterns in order to accurately anticipate future changes, it is common to classify glaciers into distinct categories based on seasonal velocity patterns (Moon et al., 2014). Depending on the year, Helheim Glacier is either runoff-driven or terminus-driven. Poinar (2023) classified Helheim as terminus-driven based on decomposition of multi-year velocity time series. Cheng et al. (2022) demonstrated through modeling that terminus position alone successfully explains observed near-terminus velocity patterns, while Ultee et al. (2022) concluded that runoff controls Helheim velocity patterns, and that changes in terminus position are in fact due to upstream changes attributed to runoff. Diurnal velocity changes at Helheim have been linked to surface melt (Stevens et al., 2022a), and Stevens et al. (2022b) found evidence of an efficient summertime drainage system in the main trunk such that the velocity pulse resulting from a supraglacial lake drainage did not yield any significant effect on ice discharge at the terminus. Each of these studies takes a separate vantage point and strategy for assessing the flow type and attribution of Helheim. Our study reframes the question as: *Where are the regions of influence of terminus effects and hydrology effects that combine to determine the overall behavior of Helheim?*

Based on our hydrology- and terminus-forced simulation results above, terminus effects dominate seasonal velocity patterns at Helheim Glacier (and likely other tidewater glaciers) in the near-terminus region, extending a strong influence on ice velocity about 15 km inland in this case. According to our coupled model, seasonal runoff is responsible for less than 10% of the ice velocity variability near the terminus. Beyond 15 km from the terminus, however, meltwater reaching the bed is the main driver of ice velocity variations, and its influence on seasonal velocity increases with enhanced melt (Figure 2).

Our model-based finding of terminus control within 15 km is consistent with observational studies (Moon et al., 2014; Vijay et al., 2019; Poinar, 2023); a small test sample of ITS.LIVE velocities also support this (Figure S10). Our finding of runoff control farther upstream is less consistent with those previous observations but the signal-to-noise ratio of the current generation of velocity products in slow-moving areas limits the ability of such observations to resolve the modeled effect (Poinar & Andrews, 2021). To answer our reframed question, on the scale of an entire outlet glacier catchment, model-based analyses are the best current path forward.

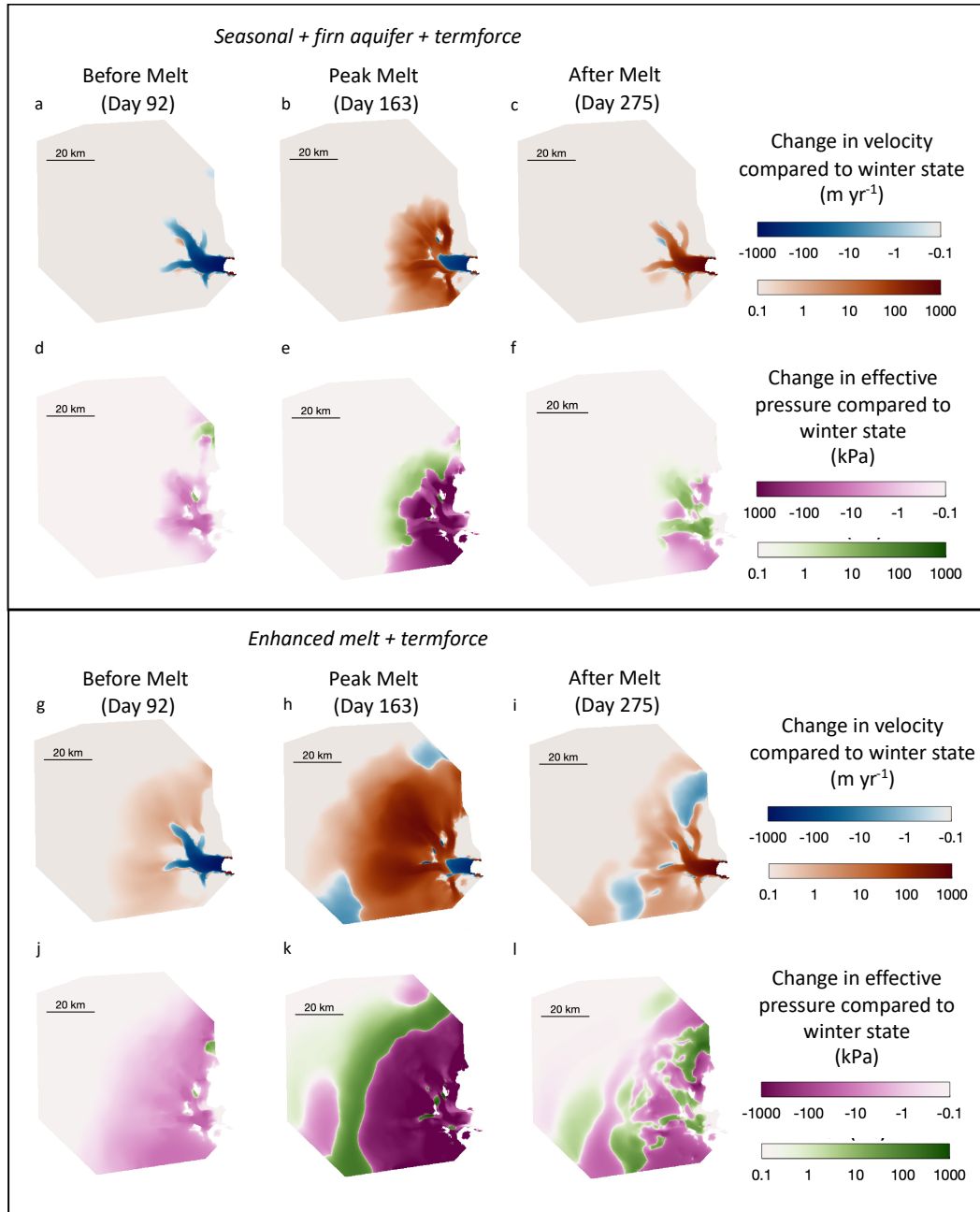


**Figure 3.** (a)-(c): Change in sliding velocity relative to winter state in *seasonal+firn aquifer+termforce* simulation on April 2 (day 92), June 12 (day 163), and October 2 (day 275), days of minimum terminus velocity (a), peak meltwater input (b), and maximum terminus velocity (c). Change in effective pressure relative to winter state on April 2 (d), June 12 (e), and October 2 (f). (g)-(l): Same for *enhanced melt+termforce* simulation.

## 4.2 Importance of hydrology-driven velocity variations of tidewater glaciers in future climate

The *enhanced melt* simulations (both with and without terminus forcing) reflect future warming scenarios where melt increases at the surface of the Greenland Ice Sheet will increase the volume of liquid water being drained to the bed at higher elevations farther inland from the ice margin. The *enhanced melt* simulations indicate hydrology will likely play a heightened role in influencing tidewater outlet glacier behavior, driving changes stemming from interior regions of the ice sheet. Although changes in ice thickness are not modeled here, acceleration in the interior could lead to greater mass loss and thinning. Moreover, as tidewater glaciers undergo substantial retreat (Williams et al., 2021), potentially transitioning into land-terminating glaciers (Aschwanden et al., 2019), we anticipate a corresponding alteration in their seasonal dynamics to one predominantly influenced by hydrological variations.

## 5 Conclusions

Through seasonal simulations of Helheim Glacier forced by meltwater inputs to the bed and by velocity changes at the terminus using the coupled hydrology–ice dynamics model SHAKTI-ISSM, we demonstrate the importance of terminus forcing up to 15 km from the terminus. Hydrology, however, determines temporal patterns of velocity upstream of that limit. In lieu of classifying tidewater glaciers as terminus-driven or hydrology-driven, we emphasize the distinct spatial realms of influence, and show that hydrologic forcing may play a heightened role in tidewater glacier future behavior as the magnitude and spatial extent of melt increases on the Greenland Ice Sheet, with widespread acceleration in the interior.

Two-way coupled modeling is necessary to capture the nuances of the nonlinear relationship between sliding velocity and effective pressure. By simulating nonlocal effects and spatiotemporal variations, SHAKTI-ISSM holds promise for further compelling work to untangle the intricacies of subglacial drainage and ice movement.

## 6 Open Research

ISSM (including SHAKTI) is freely available for download at <https://issm.jpl.nasa.gov/>. Model output data for simulations performed in this study are available in a Zenodo repository (doi: 10.5281/zenodo.10795179). Plots in this paper make use of the Scientific Colour Maps developed by Crameri (2021).

## Acknowledgments

This study was supported by the Heising-Simons Foundation (grant # 2020-1911). We also thank Jessica Badgeley, Cheng Gong, Matt Hoffman, and Ian Hewitt for helpful conversations that informed and shaped this work.

## References

- Arnold, N., & Sharp, M. (2002). Flow variability in the scandinavian ice sheet: modelling the coupling between ice sheet flow and hydrology. *Quaternary Science Reviews*, 21(4-6), 485–502. doi: 10.1016/S0277-3791(01)00059-2
- Aschwanden, A., Fahnestock, M. A., Truffer, M., Brinkerhoff, D. J., Hock, R., Khroulev, C., ... Khan, S. A. (2019). Contribution of the greenland ice sheet to sea level over the next millennium. *Science Advances*, 5(6), eaav9396. doi: 10.1126/sciadv.aav9396
- Budd, W., Keage, P., & Blundy, N. (1979). Empirical studies of ice sliding. *Journal*

- of *Glaciology*, 23(89), 157–170. doi: 10.3189/S0022143000029804
- Cheng, G., Morlighem, M., Mouginot, J., & Cheng, D. (2022). Helheim glacier’s terminus position controls its seasonal and inter-annual ice flow variability. *Geophysical Research Letters*, 49(5), e2021GL097085. doi: 10.1029/2021GL097085
- Cook, S. J., Christoffersen, P., & Todd, J. (2022). A fully-coupled 3d model of a large greenlandic outlet glacier with evolving subglacial hydrology, frontal plume melting and calving. *Journal of Glaciology*, 68(269), 486–502. doi: 10.1017/jog.2021.109
- Cook, S. J., Christoffersen, P., Todd, J., Slater, D., & Chauché, N. (2020). Coupled modelling of subglacial hydrology and calving-front melting at store glacier, west greenland. *The Cryosphere*, 14(3), 905–924. doi: 10.5194/tc-14-905-2020
- Crameri, F. (2021). Scientific colour maps (7.0.1). *Zenodo*. doi: 10.5281/zenodo.5501399
- de Fleurian, B., Werder, M. A., Beyer, S., Brinkerhoff, D. J., Delaney, I., Dow, C. F., ... others (2018). Shmip the subglacial hydrology model intercomparison project. *Journal of Glaciology*, 64(248), 897–916. doi: 10.1017/jog.2018.78
- Dias dos Santos, T., Morlighem, M., & Brinkerhoff, D. (2022). A new vertically integrated mono-layer higher-order (molho) ice flow model. *The Cryosphere*, 16(1), 179–195. doi: 10.5194/tc-16-179-2022
- Drew, M., & Tarasov, L. (2023). Surging of a hudson strait-scale ice stream: subglacial hydrology matters but the process details mostly do not. *The Cryosphere*, 17(12), 5391–5415. doi: 10.5194/tc-17-5391-2023
- Ehrenfeucht, S., Morlighem, M., Rignot, E., Dow, C. F., & Mouginot, J. (2023). Seasonal acceleration of petermann glacier, greenland, from changes in subglacial hydrology. *Geophysical Research Letters*, 50(1), e2022GL098009. doi: 10.1029/2022GL098009
- Enderlin, E. M., Hamilton, G. S., O’Neel, S., Bartholomaus, T. C., Morlighem, M., & Holt, J. W. (2016). An empirical approach for estimating stress-coupling lengths for marine-terminating glaciers. *Frontiers in Earth Science*, 4, 104. doi: 10.3389/feart.2016.00104
- Flowers, G. E. (2015). Modelling water flow under glaciers and ice sheets. *Proceedings of the Royal Society A: Mathematical, Physical and Engineering Sciences*, 471(2176), 20140907. doi: 10.1098/rspa.2014.0907
- Gagliardini, O., & Werder, M. A. (2018). Influence of increasing surface melt over decadal timescales on land-terminating greenland-type outlet glaciers. *Journal of Glaciology*, 64(247), 700–710. doi: 10.1017/jog.2018.59
- GMAO. (2015). *Merra-2 tavg1-2d\_lnd\_nx: 2d,1-hourly,time-averaged,single-level,assimilation,land surface diagnostics v5.12.4*. Global Modeling and Assimilation Office, Greenbelt, MD, USA, Goddard Earth Sciences Data and Information Services Center (GES DISC), Accessed: January 6, 2022.
- Hewitt, I. (2013). Seasonal changes in ice sheet motion due to melt water lubrication. *Earth and Planetary Science Letters*, 371, 16–25. doi: 10.1016/j.epsl.2013.04.022
- Hill, T., Flowers, G. E., Hoffman, M. J., Bingham, D., & Werder, M. A. (2023). Improved representation of laminar and turbulent sheet flow in subglacial drainage models. *Journal of Glaciology*, 1–14. doi: 10.1017/jog.2023.103
- Hoffman, M., & Price, S. (2014). Feedbacks between coupled subglacial hydrology and glacier dynamics. *Journal of Geophysical Research: Earth Surface*, 119(3), 414–436. doi: 10.1002/2013JF002943
- Joughin, I., Smith, B. E., & Howat, I. M. (2018). A complete map of greenland ice velocity derived from satellite data collected over 20 years. *Journal of Glaciology*, 64(243), 1–11. doi: 10.1017/jog.2017.73
- Kingslake, J., & Ng, F. (2013). Modelling the coupling of flood discharge with

- glacier flow during jökulhlaups. *Annals of Glaciology*, 54(63), 25–31. doi: 10.3189/2013AoG63A331
- Larour, E., Seroussi, H., Morlighem, M., & Rignot, E. (2012). Continental scale, high order, high spatial resolution, ice sheet modeling using the ice sheet system model (issm). *Journal of Geophysical Research: Earth Surface*, 117(F1). doi: 10.1029/2011JF002140
- Lu, G., & Kingslake, J. (2023). Coupling between ice flow and subglacial hydrology enhances marine ice-sheet retreat. *EGU sphere*, 2023, 1–31. doi: 10.5194/egusphere-2023-2794
- Mankoff, K. D., Solgaard, A., Colgan, W., Ahlstrøm, A. P., Khan, S. A., & Fausto, R. S. (2020). Greenland ice sheet solid ice discharge from 1986 through march 2020. *Earth System Science Data*, 12(2), 1367–1383. doi: 10.5194/essd-12-1367-2020
- Miège, C., Forster, R. R., Brucker, L., Koenig, L. S., Solomon, D. K., Paden, J. D., ... others (2016). Spatial extent and temporal variability of greenland firn aquifers detected by ground and airborne radars. *Journal of Geophysical Research: Earth Surface*, 121(12), 2381–2398. doi: 10.1002/2016JF003869
- Minchew, B. M., Meyer, C. R., Pegler, S. S., Lipovsky, B. P., Rempel, A. W., Gudmundsson, G. H., & Iverson, N. R. (2019). Comment on “friction at the bed does not control fast glacier flow”. *Science*, 363(6427), eaau6055. doi: 10.1126/science.aau6055
- Moon, T., Joughin, I., Smith, B., Van Den Broeke, M. R., Van De Berg, W. J., Noël, B., & Usher, M. (2014). Distinct patterns of seasonal Greenland glacier velocity. *Geophysical Research Letters*, 41(20), 7209–7216. doi: 10.1002/2014GL061836
- Morlighem, M., et al. (2021). Icebridge bedmachine greenland, version 4 [data set]. *NASA National Snow and Ice Data Center Distributed Active Archive Center*. doi: 10.5067/VLJ5YXKCNGXO
- Mouginot, J., Rignot, E., Björk, A. A., Van den Broeke, M., Millan, R., Morlighem, M., ... Wood, M. (2019). Forty-six years of Greenland Ice Sheet mass balance from 1972 to 2018. *Proceedings of the National Academy of Sciences*, 116(19), 9239–9244. doi: 10.1073/pnas.1904242116
- Pimentel, S., & Flowers, G. E. (2011). A numerical study of hydrologically driven glacier dynamics and subglacial flooding. *Proceedings of the Royal Society A: Mathematical, Physical and Engineering Sciences*, 467(2126), 537–558. doi: 10.1098/rspa.2010.0211
- Poinar, K. (2023). Seasonal flow types of glaciers in Sermilik Fjord, Greenland, over 2016–2021. *Journal of Geophysical Research: Earth Surface*, 128(7), e2022JF006901. doi: 10.1029/2022JF006901
- Poinar, K., & Andrews, L. C. (2021). Challenges in predicting Greenland supraglacial lake drainages at the regional scale. *The Cryosphere*, 15(3), 1455–1483. doi: 10.5194/tc-15-1455-2021
- Poinar, K., Dow, C. F., & Andrews, L. C. (2019). Long-term support of an active subglacial hydrologic system in Southeast Greenland by firn aquifers. *Geophysical Research Letters*, 46(9), 4772–4781. doi: 10.1029/2019GL082786
- Sommers, A., Meyer, C., Morlighem, M., Rajaram, H., Poinar, K., Chu, W., & Mejia, J. (2023). Subglacial hydrology modeling predicts high winter water pressure and spatially variable transmissivity at Helheim Glacier, Greenland. *Journal of Glaciology*, 1–13. doi: 10.1017/jog.2023.39
- Sommers, A., Rajaram, H., & Morlighem, M. (2018). SHAKTI: subglacial hydrology and kinetic, transient interactions v1. 0. *Geoscientific Model Development*, 11(7), 2955–2974. doi: 10.5194/gmd-11-2955-2018
- Stevens, L. A., Hewitt, I. J., Das, S. B., & Behn, M. D. (2018). Relationship between Greenland Ice Sheet surface speed and modeled effective pressure. *Journal of Geophysical Research: Earth Surface*, 123(9), 2258–2278. doi: 10.1029/



2017JF004581

Stevens, L. A., Nettles, M., Davis, J. L., Creyts, T. T., Kingslake, J., Ahlstrøm, A. P., & Larsen, T. B. (2022a). Helheim Glacier diurnal velocity fluctuations driven by surface melt forcing. *Journal of Glaciology*, 68(267), 77–89. doi: 10.1017/jog.2021.74

Stevens, L. A., Nettles, M., Davis, J. L., Creyts, T. T., Kingslake, J., Hewitt, I. J., & Stubblefield, A. (2022b). Tidewater-glacier response to supraglacial lake drainage. *Nature Communications*, 13(1), 6065.

Ultee, L., Felikson, D., Minchew, B., Stearns, L. A., & Riel, B. (2022). Helheim Glacier ice velocity variability responds to runoff and terminus position change at different timescales. *Nature Communications*, 13(1), 6022. doi: 10.1038/s41467-022-33292-y

Vijay, S., Khan, S. A., Kusk, A., Solgaard, A. M., Moon, T., & Bjørk, A. A. (2019). Resolving seasonal ice velocity of 45 Greenlandic glaciers with very high temporal details. *Geophysical Research Letters*, 46(3), 1485–1495. doi: 10.1029/2018GL081503

Williams, J. J., Gourmelen, N., Nienow, P., Bunce, C., & Slater, D. (2021). Helheim glacier poised for dramatic retreat. *Geophysical Research Letters*, 48(23), e2021GL094546. doi: 10.1029/2021GL094546